Structural Phase Transition and Crystal Structure for $(ND_4)_4D_2(SeO_4)_3$ at Low Temperature

T. FUKAMI*

Department of Physics and Earth Sciences, Faculty of Science
University of the Ryukyus, Okinawa 903-0213, Japan

AND R.H. CHEN

Department of Physics, National Taiwan Normal University
Taipei, Taiwan, 117, Republic of China

(Received May 14, 2001)

Differential scanning calorimetry and X-ray diffraction measurements were performed on a deuterated tetraammonium dihydrogen triselenate $(ND_4)_4D_2(SeO_4)_3$ crystal at low temperatures. A structural phase transition is found at 182.0(3) K. The space group symmetry (triclinic $P1$) and the structure parameters are determined at 145 K in the low-temperature phase. The isotope effect for an asymmetric O–H–O hydrogen bond by the substitution of deuterium is discussed.

PACS numbers: 61.66.Fn, 64.60.Fr

1. Introduction

Tetraammonium dihydrogen triselenate $(NH_4)_4H_2(SeO_4)_3$ crystal exhibits a superionic phase transition at 378 K and melts at 432 K as observed by thermal and electrical conductivity measurements [1, 2]. A substantial increase in electrical conductivity from 10^{-5} to 4×10^{-3} Ω^{-1} cm^{-1} occurs at the transition [2]. The high-temperature phase is recognized as the superionic state with a low activation energy (0.11 eV) [2–7]. It is found from the Raman measurements that a change

*corresponding author; e-mail: fukami@sci.u-ryukyu.ac.jp

in dynamics of SeO_4 and $HSeO_4$ entities begins about 15 K below the superionic transition temperature and the temperature hysteresis of its transition temperature is about 30 K [6, 7]. The crystal structure at room temperature is found to be triclinic with space group $P\bar{1}$ with two molecular units in a unit cell [1, 8].

In the previous papers [9, 10] we have performed differential scanning calorimetry (DSC), electron paramagnetic resonance (EPR) and X-ray diffraction measurements for the $(NH_4)_4H_2(SeO_4)_3$ crystal below room temperature. The DSC curve and the temperature dependence of the ^{77}Se hyperfine line positions of a SeO_3^- radical show the existence of a low-temperature structural phase transition at 182 K. Moreover, the crystal structure at 141 K in the low-temperature phase is found to be triclinic with space group $P1$ [10]. The position of the O(1) atom of a $Se(1)O_4$ tetrahedron is shifted during the transition from the room- to the low-temperature phases. As viewed along the direction which is perpendicular to the two mutually perpendicular bonds of O(1)–O(4) and O(2)–O(3), the angle of the deviation of the O(1) atom from the Se–O(1) direction is about 6° [10].

On the other hand, a deuterated tetraammonium dihydrogen triselenate $(ND_4)_4D_2(SeO_4)_3$ crystal exhibits high-temperature phase transitions at 378 K and 428 K, and melts at 432 K as observed by DSC measurements [1]. The crystal structure for the $(ND_4)_4D_2(SeO_4)_3$ crystal at room temperature is found to be triclinic with space group $P\bar{1}$ [1]. However, the crystal structure and the existence of phase transition at low temperature have not been reported yet. The purpose of this paper is to reveal the existence of the low-temperature structural phase transition of $(ND_4)_4D_2(SeO_4)_3$ by differential scanning calorimetry and to report the crystal structure in the low-temperature phase.

2. Experimental

Single crystals of $(ND_4)_4D_2(SeO_4)_3$ were recrystallized six times from a D_2O solution containing deuterated crystals, by slow evaporation in a desiccator over P_2O_5. The first deuterated crystals were obtained from a D_2O solution containing $(NH_4)_2SeO_4$ and H_2SeO_4 at the molar ratio of 1.44 : 1 by the evaporation method [1]. No signals from H nuclei in the sample crystal were observed by the Fourier transform NMR (FT-NMR) measurements. Therefore, the deuteration rate of the sample crystals is considered to be nearly 100%.

Differential scanning calorimetry (DSC) was performed with a DSC220 from Seiko Instruments, Inc. The amounts of the sample crystal for the DSC measurement varied between 1.64 and 6.25 mg. The X-ray measurement was carried out by using an Enraf-Nonius CAD-4 four-circle automatic diffractometer with an express software and graphite monochromated Mo K_α radiation (λ = 0.71073 Å). The sample temperature was controlled by using cold N_2 gas with a low-temperature apparatus of Enraf-Nonius, and the temperature fluctuation was kept within ±0.5 K. The intensity data were corrected for both Lorentz-polarization

and absorption effects. The structure was refined by the full-matrix least square method using an SDP crystallographic software package on a personal computer

TABLE I

Basic crystallographic data, data collection and structure refinement parameters.

Crystal data	
Compound/chemical formula weight	$(ND_4)_4D_2(SeO_4)_3/M_r = 521.15$
Crystal system/space group	Triclinic/$P1$
Lattice constants	$a = 7.650(1)$ Å, $\alpha = 114.34(1)°$
	$b = 10.336(2)$ Å, $\beta = 93.29(1)°$
	$c = 10.509(2)$ Å,
$\gamma = 107.54(1)°$	
Volume of unit cell	$V = 706.0(2)$ Å^3
Formula unit per cell	$Z = 2$
Calculated density	$D_x = 2.452$ mg m^{-3}
Linear absorption coefficient	$\mu = 7.88$ mm^{-1}
Crystal shape/colour	Prism/colourless
Sample shape/size in diameter	Sphere/$2r = 0.31$ mm
Data collection	
Measurement of temperature	145 K
Data-collection method	$\theta/2\theta$ scans
Absorption correction type	Spherical
Number of reflections measured	6473 ($\theta_{max} = 35.0°$)
Range of h, k, and l for measured intensities	$h = -11 \rightarrow 12$
	$k = -16 \rightarrow 0$
	$l = -15 \rightarrow 16$
Number of standard reflections	3
Interval time/intensity decay	120 min/–1.21%
Refinement	
R factor/wR factor (refinement on F)	$R = 0.030/wR = 0.049$
Goodness of fit	$S = 1.602$
Number of reflections used in refinement	4745 ($I > 3\sigma(I)$)
Number of parameters refined	488
Weighting scheme	$w = 1/[\sigma^2(F) + (0.02F)^2 + 1.0]$
Maximum of shift/esd	$(\Delta/\sigma)_{max} = 0.10$
Difference density (peak/hole)	0.861/–1.553 e Å^{-3}
Extinction coefficient	$7.5(5) \times 10^{-7}$

[11]. All nonhydrogen atoms were refined with anisotropic thermal parameters and the hydrogen atoms involved in hydrogen O...O bonds were refined isotropically.

However, the isotropic thermal parameter of the hydrogen atoms of the ND_4 ions was fixed with 0.02. Basic crystallographic data and the experimental conditions are listed in Table I.

3. Results and discussion

Figure 1 shows the DSC heating curves for the proton and deuterated compounds below room temperature. The heating rates for the proton and deuterated compounds were 10 K min^{-1}. The weak endothermic peaks shown by the arrows are detected in the DSC charts. Generally, a peak in the DSC chart suggests the exchange energy at a phase transition. The existence of the phase transition in the proton compound has been confirmed by the EPR measurements [9]. Therefore, we consider that the weak peak appeared in the chart for the deuterated compound also indicates the existence of a phase transition. The phase transition temperatures are chosen at the peak temperature of the DSC curve at which the phase transition becomes complete. The averaged temperature of the phase transition for some samples is determined to be 182(1) K for the proton compound and 182.0(3) K for the deuterated compound [9]. Then, these results indicate that the substitution of deuterium for hydrogen in hydrogen bonds does not affect the transition temperature in this crystal. The transition enthalpy ΔH (entropy ΔS) at the peak is determined to be 0.8(1) kJ mol^{-1} (4.5(6) J K^{-1} mol^{-1}) for the proton compound and 0.52(5) kJ mol^{-1} (2.9(3) J K^{-1} mol^{-1}) for the deuterated compound [9].

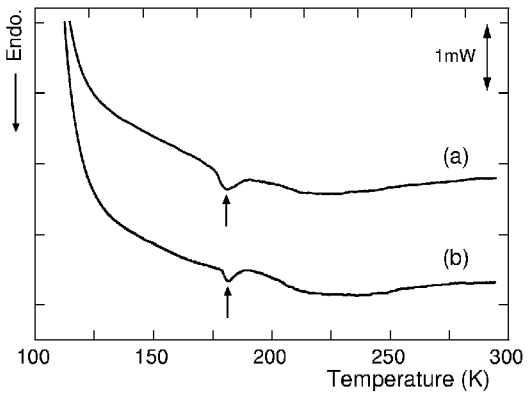

Fig. 1. DSC curves for (a) $(NH_4)_4H_2(SeO_4)_3$ and (b) $(ND_4)_4D_2(SeO_4)_3$ crystals on heating [9]. The sample weights for the $(NH_4)_4H_2(SeO_4)_3$ and $(ND_4)_4D_2(SeO_4)_3$ crystals were 5.52 and 6.25 mg, respectively. The heating rates were 10 K min^{-1}.

The structure of the $(ND_4)_4D_2(SeO_4)_3$ crystal at 145 K in the low-temperature phase was analyzed by X-ray diffraction. The observed lattice parameters are very close to those obtained at room temperature except small crystal shortening along the a- and b-axes [1]. No systematic absence can be found for the observed reflections, similarly to those at room temperature. Therefore, the space group is proposed to be triclinic $P\bar{1}$ or $P1$. The discrepancy factors (R factors) for the structure analysis calculated for both the space groups were all reduced to about 0.03. However, the obtained atomic positions in the $P\bar{1}$ structure are almost the same as those in the room-temperature phase except the small shifts of the atomic positions produced by the changes of the lattice parameters. This would exclude the phase transition. Therefore, the space group in the low-temperature phase is considered to be $P1$.

The positional parameters in fractions of the unit cell and the thermal parameters are listed in Table II. Selected bond lengths in Å and bond angles in degrees are given in Table III.

TABLE II

Positional parameters in fractions of the unit cell, equivalent isotropic U_{eq} (Se, O, and N) or isotropic U_{iso} (D) thermal parameters (Å^2) at 145 K, where $U_{eq} = (1/3)\sum_i \sum_j U_{ij} a_i^* a_j^* \boldsymbol{a}_i \cdot \boldsymbol{a}_j$. The isotropic thermal parameter of the D atoms around the ND_4 ions was fixed with $U_{iso} = 0.02$.

Atom	X	Y	Z	U_{eq}/U_{iso}
Se(1)	0.15414	0.72894	0.36661	0.0383(2)
Se(2)	0.45600(8)	0.62927(6)	0.72820(6)	0.0251(2)
Se(3)	0.16911(8)	0.13101(6)	0.88513(6)	0.0200(2)
Se(4)	0.85559(8)	0.26982(6)	0.63370(5)	0.0295(2)
Se(5)	0.54858(8)	0.36372(6)	0.26915(6)	0.0248(2)
Se(6)	0.83797(9)	0.86261(6)	0.11128(6)	0.0211(2)
O(1)	0.3457(6)	0.8387(5)	0.3451(5)	0.049(1)
O(2)	0.0440(9)	0.5538(6)	0.2224(6)	0.041(2)
O(3)	0.0011(7)	0.8142(5)	0.3899(5)	0.062(1)
O(4)	0.1990(7)	0.7040(5)	0.5053(4)	0.047(1)
O(5)	0.5112(7)	0.5091(5)	0.7633(5)	0.036(2)
O(6)	0.3454(6)	0.7236(6)	0.8390(6)	0.048(2)
O(7)	0.2964(7)	0.5144(5)	0.5651(5)	0.027(2)
O(8)	0.6332(7)	0.7562(5)	0.7110(5)	0.044(1)

TABLE II (cont.)

Atom	X	Y	Z	U_{eq}/U_{iso}
O(9)	0.3394(7)	0.2544(5)	0.8598(5)	0.035(2)
O(10)	0.2301(8)	0.0245(6)	0.9370(5)	0.048(2)
O(11)	0.0453(6)	0.2234(5)	0.9833(4)	0.028(1)
O(12)	0.0106(8)	0.0063(6)	0.7208(5)	0.032(2)
O(13)	0.6684(8)	0.1843(6)	0.6713(6)	0.068(2)
O(14)	0.9402(7)	0.4297(5)	0.7672(5)	0.038(2)
O(15)	0.9853(7)	0.1625(5)	0.5943(5)	0.044(2)
O(16)	0.7975(7)	0.2847(6)	0.4872(5)	0.051(2)
O(17)	0.4744(7)	0.4814(5)	0.2357(5)	0.046(2)
O(18)	0.6597(6)	0.2852(5)	0.1555(4)	0.026(1)
O(19)	0.6945(6)	0.4755(5)	0.4333(5)	0.031(1)
O(20)	0.3834(6)	0.2452(5)	0.2980(5)	0.022(1)
O(21)	0.6607(7)	0.7487(5)	0.1362(5)	0.039(2)
O(22)	0.7675(7)	0.9785(5)	0.0699(5)	0.042(2)
O(23)	0.9608(8)	0.7830(7)	0.0128(6)	0.056(2)
O(24)	0.9748(7)	0.9867(5)	0.2739(5)	0.020(1)
N(1)	0.2804(8)	0.5398(5)	0.0122(5)	0.037(2)
N(2)	0.3853(9)	0.9446(6)	0.1360(5)	0.037(2)
N(3)	0.0240(6)	0.2928(5)	0.2749(5)	0.025(1)
N(4)	0.3535(9)	0.2133(7)	0.5488(6)	0.060(2)
N(5)	0.7312(7)	0.4682(6)	0.9946(6)	0.032(2)
N(6)	0.6424(8)	0.0629(6)	0.8667(6)	0.056(2)
N(7)	0.9864(8)	0.7120(6)	0.7250(6)	0.023(2)
N(8)	0.6551(8)	0.7999(8)	0.4562(6)	0.053(2)
D(O1)	1.00(2)	0.10(1)	0.68(1)	0.02(3)
D(O2)	0.27(2)	0.60(1)	0.54(1)	0.02(3)
D(O3)	0.98(2)	0.95(1)	0.31(1)	0.02(3)
D(O4)	0.72(2)	0.44(1)	0.45(1)	0.02(3)
D(1)	0.31(2)	0.47(1)	–0.03(1)	0.02
D(2)	0.21(2)	0.54(1)	–0.05(1)	0.02

TABLE II (cont.)

Atom	X	Y	Z	U_{eq}/U_{iso}
D(3)	0.37(2)	0.61(1)	0.05(1)	0.02
D(4)	0.21(2)	0.52(1)	0.06(1)	0.02
D(5)	0.35(2)	0.90(1)	0.21(1)	0.02
D(6)	0.47(2)	0.93(1)	0.09(1)	0.02
D(7)	0.40(2)	1.04(1)	0.19(1)	0.02
D(8)	0.25(2)	0.89(1)	0.08(1)	0.02
D(9)	0.01(2)	0.20(1)	0.20(1)	0.02
D(10)	0.01(2)	0.36(1)	0.26(1)	0.02
D(11)	–0.03(2)	0.30(1)	0.35(1)	0.02
D(12)	0.12(2)	0.29(1)	0.28(1)	0.02
D(13)	0.42(2)	0.16(1)	0.58(1)	0.02
D(14)	0.36(2)	0.21(1)	0.46(1)	0.02
D(15)	0.43(2)	0.31(1)	0.63(1)	0.02
D(16)	0.22(2)	0.17(1)	0.55(1)	0.02
D(17)	0.72(2)	0.58(1)	1.07(1)	0.02
D(18)	0.76(2)	0.44(1)	1.05(1)	0.02
D(19)	0.62(2)	0.39(1)	0.95(1)	0.02
D(20)	0.78(2)	0.46(1)	0.92(1)	0.02
D(21)	0.62(2)	0.08(1)	0.82(1)	0.02
D(22)	0.51(2)	0.05(1)	0.88(1)	0.02
D(23)	0.63(2)	–0.02(1)	0.84(1)	0.02
D(24)	0.73(2)	0.11(1)	0.93(1)	0.02
D(25)	1.08(2)	0.78(1)	0.80(1)	0.02
D(26)	1.00(2)	0.64(1)	0.74(1)	0.02
D(27)	1.02(2)	0.70(1)	0.65(1)	0.02
D(28)	0.86(2)	0.73(1)	0.73(1)	0.02
D(29)	0.60(2)	0.85(1)	0.44(1)	0.02
D(30)	0.65(2)	0.79(1)	0.52(1)	0.02
D(31)	0.63(2)	0.75(1)	0.40(1)	0.02
D(32)	0.77(2)	0.81(1)	0.43(1)	0.02

TABLE III

Selected bond lengths in Å (a) and bond angles in degrees (b) at 145 K.

(a) Bond lengths

Se(1)–O(1)	1.653(5)	Se(4)–O(13)	1.606(6)
Se(1)–O(2)	1.720(4)	Se(4)–O(14)	1.568(4)
Se(1)–O(3)	1.638(6)	Se(4)–O(15)	1.648(6)
Se(1)–O(4)	1.617(5)	Se(4)–O(16)	1.658(6)
Se(2)–O(5)	1.592(7)	Se(5)–O(17)	1.634(6)
Se(2)–O(6)	1.642(6)	Se(5)–O(18)	1.594(5)
Se(2)−O(7)	1.745(4)	Se(5)–O(19)	1.707(4)
Se(2)–O(8)	1.656(5)	Se(5)–O(20)	1.614(5)
Se(3)–O(9)	1.647(5)	Se(6)–O(21)	1.620(5)
Se(3)–O(10)	1.582(7)	Se(6)–O(22)	1.646(7)
Se(3)–O(11)	1.649(5)	Se(6)–O(23)	1.583(7)
Se(3)−O(12)	1.760(4)	Se(6)–O(24)	1.685(4)
O(1)–O(2)	2.845(6)	O(13)–O(14)	2.499(6)
O(1)–O(3)	2.659(7)	O(13)–O(15)	2.643(8)
O(1)–O(4)	2.691(8)	O(13)–O(16)	2.655(9)
O(2)–O(3)	2.673(8)	O(14)–O(15)	2.749(7)
O(2)–O(4)	2.709(7)	O(14)–O(16)	2.666(6)
O(3)–O(4)	2.651(9)	O(15)–O(16)	2.647(9)
O(5)–O(6)	2.741(9)	O(17)–O(18)	2.700(8)
O(5)–O(7)	2.607(8)	O(17)–O(19)	2.629(8)
O(5)–O(8)	2.734(8)	O(17)–O(20)	2.686(8)
O(6)–O(7)	2.713(6)	O(18)–O(19)	2.706(6)
O(6)–O(8)	2.652(7)	O(18)–O(20)	2.688(7)
O(7)–O(8)	2.782(6)	O(19)–O(20)	2.600(5)
O(9)–O(10)	2.734(9)	O(21)–O(22)	2.657(8)
O(9)–O(11)	2.664(7)	O(21)–O(23)	2.703(9)
O(9)–O(12)	2.764(6)	O(21)–O(24)	2.650(6)
O(10)–O(11)	2.733(9)	O(22)–O(23)	2.746(10)
O(10)–O(12)	2.653(9)	O(22)–O(24)	2.550(8)
O(11)–O(12)	2.679(6)	O(23)–O(24)	2.654(7)

TABLE III (cont.)

(a) Bond lengths			
O(3)–O(24)	2.585(9)	O(12)–O(15)	2.517(9)
O(3)–D(O3)	1.88(15)	O(12)–D(O1)	1.23(15)
D(O3)–O(24)	0.71(15)	D(O1)–O(15)	1.32(15)
O(4)–O(7)	2.575(9)	O(16)–O(19)	2.576(9)
O(4)–D(O2)	1.47(15)	O(16)−D(O4)	1.98(15)
D(O2)–O(7)	1.11(14)	D(O4)–O(19)	0.60(15)
(b) Bond angles			
O(1)–Se(1)–O(2)	115.0(3)	O(13)–Se(4)−O(14)	103.9(3)
O(1)–Se(1)–O(3)	107.8(3)	O(13)–Se(4)–O(15)	108.6(3)
O(1)–Se(1)–O(4)	110.7(2)	O(13)–Se(4)–O(16)	108.9(3)
O(2)–Se(1)–O(3)	105.5(3)	O(14)–Se(4)–O(15)	117.4(3)
O(2)–Se(1)–O(4)	108.5(3)	O(14)–Se(4)−O(16)	111.4(3)
O(3)–Se(1)–O(4)	109.1(3)	O(15)–Se(4)–O(16)	106.4(3)
O(5)–Se(2)–O(6)	115.9(3)	O(17)–Se(5)–O(18)	113.5(3)
O(5)–Se(2)–O(7)	102.7(2)	O(17)–Se(5)–O(19)	103.8(2)
O(5)–Se(2)–O(8)	114.7(3)	O(17)–Se(5)−O(20)	111.6(3)
O(6)–Se(2)–O(7)	106.4(2)	O(18)–Se(5)–O(19)	110.1(2)
O(6)–Se(2)–O(8)	107.1(3)	O(18)–Se(5)–O(20)	113.9(2)
O(7)–Se(2)–O(8)	109.7(2)	O(19)–Se(5)–O(20)	103.0(2)
O(9)–Se(3)–O(10)	115.7(3)	O(21)–Se(6)−O(22)	108.9(3)
O(9)–Se(3)–O(11)	107.8(3)	O(21)–Se(6)–O(23)	115.0(3)
O(9)–Se(3)–O(12)	108.4(3)	O(21)–Se(6)–O(24)	106.5(2)
O(10)–Se(3)–O(11)	115.5(3)	O(22)–Se(6)–O(23)	116.5(4)
O(10)–Se(3)–O(12)	105.0(3)	O(22)–Se(6)–O(24)	99.9(2)
O(11)–Se(3)–O(12)	103.5(2)	O(23)–Se(6)–O(24)	108.5(3)
O(3)–D(O3)–O(24)	173(11)	O(12)–D(O1)–O(15)	160(9)
O(4)–D(02)−O(7)	171(10)	O(16)–D(O4)–O(19)	171(13)

Figure 2 shows a perspective view of the crystal structure of $(ND_4)_4D_2(SeO_4)_3$ at 145 K. The observed structure is close to the previously reported structures at room temperature of the proton and deuterated compounds, and at low temperature of the proton compound [1, 8, 10].

A comparison of the obtained Se–O bond lengths at 145 K with those obtained at room temperature for the deuterated compound is given as follows. The $Se(2)O_4$ and $Se(3)O_4$ tetrahedra in the room-temperature phase are slightly distorted from the regular ones, and the $Se(1)O_4$ tetrahedron is nearly regular. On the other hand, all SeO_4 tetrahedra in the low-temperature phase are deviated from the regular ones. The deviations at 145 K are larger than those at room

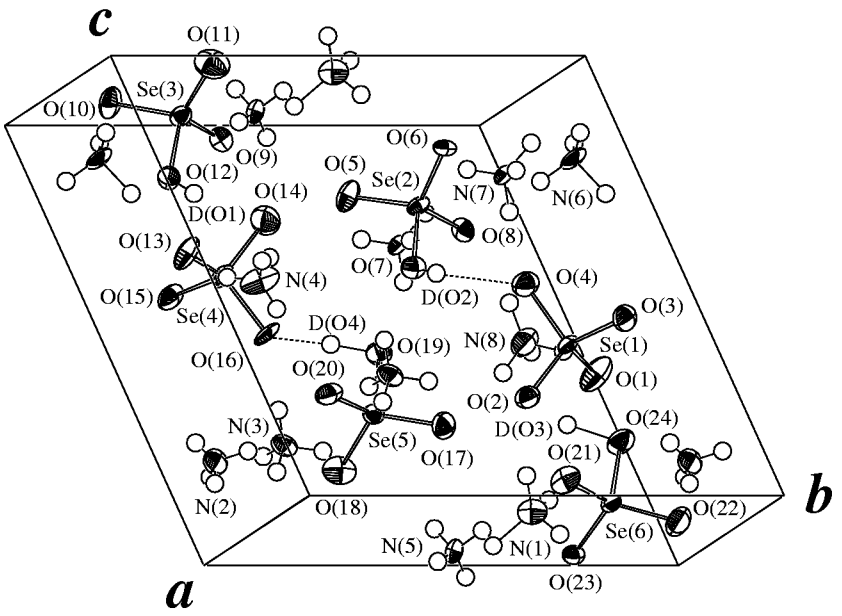

Fig. 2. Perspective view of the $(ND_4)_4D_2(SeO_4)_3$ crystal structure at 145 K with 70% probability-displacement thermal ellipsoids.

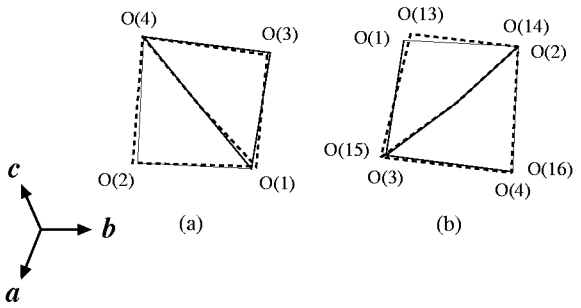

Fig. 3. Projection on the plane along the direction perpendicular to the O(1)–O(4) and O(2)–O(3) bonds for the $Se(1)O_4$ tetrahedron at room temperature. The solid lines show the $Se(1)O_4$ tetrahedra at room temperature, and the dashed lines show the (a) $Se(1)O_4$ and (b) $Se(4)O_4$ tetrahedra at 145 K. The diagonal lines indicate the lines from the position of the Se atom to those of the O atom. The angles of the deviation of the O(1) and O(13) atoms from the Se–O(1) direction of the room-temperature phase are about 3° and 6°, respectively.

temperature. The averaged O...O hydrogen bond distance at 145 K is 2.563(9) Å and is almost equal to that (2.567(7) Å) at room temperature.

In the low-temperature phase, the averaged shifts of the Se atom from the center of the O_4 tetrahedron along the *a*-, *b*-, and *c*-axes are found to be about 0.04, –0.01, and 0.01 Å for the deuterated compound, respectively. The shift for the proton compound along the *c*-axis is about –0.01 Å and along the other axes it is almost equal to the magnitude of the error of the atomic positions [10]. Therefore, the shift of the Se atom from the center is larger in the deuterated compound than in the proton compound. A schematic drawing of the $Se(1)O_4$ and $Se(4)O_4$ tetrahedra for the deuterated compound at room temperature and at 145 K is shown in Fig. 3, as viewed along the direction which is almost perpendicular to the two mutually perpendicular bonds of O(1)–O(4) and O(2)–O(3) of the $Se(1)O_4$ tetrahedron at room temperature. The two tetrahedra, $Se(1)O_4$ and $Se(4)O_4$, of the low-temperature phase correspond to the $Se(1)O_4$ tetrahedron of the room-temperature phase. The angles of the deviation of the O(1) and O(13) atoms from the Se–O(1) direction of the room-temperature phase are observed to be about 3° and 6°, respectively. One of the obtained angles is equal to that of the proton compound at 141 K. Therefore, it implies that the O(13) atom of the $Se(4)O_4$ tetrahedron is significantly shifted during the phase transition, similarly to that of the proton compound [9, 10].

On the basis of many accurate data on the crystal structures and related properties of hydrogen-bonded crystals (O–H–O bond crystals), Ichikawa pointed out that a large shift of the phase transition temperature (70 K to 100 K reported) on deuteration occurred when the hydrogen bond is symmetric with the bond length in the range of about 2.5 to 2.6 Å in the high-temperature phase [12–14]. He also showed that the shift of the phase transition temperature is about 10 K or less as the symmetric hydrogen bond length is around 2.44 Å or the hydrogen bond is asymmetric with bond distance in the range of 2.5 to 2.6 Å. It has been reported that the O–H–O hydrogen bonds of $(NH_4)_4H_2(SeO_4)_3$ in the room-temperature phase are asymmetric, and the bond lengths are between 2.546(4) and 2.554(4) Å [1]. The expansions of the O...O hydrogen bonds at room temperature by the deuteration are about 0.02 Å [1], and the shift of the transition temperature is not observed in the DSC charts. Therefore, it is clearly seen that an isotope effect on the hydrogen bond of $(NH_4)_4H_2(SeO_4)_3$ follows the Ichikawa condition which concerns the small shift of the transition temperature.

The origin of the small shift of the transition temperature for the asymmetric O–H–O hydrogen bond has not been given by Ichikawa. In the proton and deuterated compounds in the room- and low-temperature phases, the bond distance between the Se atom and the O atom ended with the O...O hydrogen bonds is longer than the other distances in the SeO_4 tetrahedra except the $Se(1)O_4$ tetrahedron which has two hydrogen bonds connected [1, 10]. The averaged magnitudes (about 0.10 Å) of the difference between the longest distance and the others in the proton compound are almost the same as those found in the deuterated compound. These results indicate that there exists a greater bonding strength between the O

atoms which are connected by the hydrogen bonds, but the bonding strength is not affected by the substitution of deuterium in spite of the fact that the expansion of the hydrogen bonds at room temperature is about 0.02 Å [1].

This is also found in the $Na_3H(SO_4)_2$ and $Na_3D(SO_4)_2$ crystal structures which contain very short asymmetric hydrogen bonds (about 2.43 Å) [15–18]. However, the averaged magnitude (about 0.05 Å) of the difference between the longest distance and the others in the SO_4 tetrahedron of the $Na_3H(SO_4)_2$ and $Na_3D(SO_4)_2$ crystals is half of the magnitude (about 0.10 Å) in the $(NH_4)_4H_2(SeO_4)_3$ and $(ND_4)_4D_2(SeO_4)_3$ crystals. This indicates that the bonding strength in the $Na_3H(SO_4)_2$ and $Na_3D(SO_4)_2$ crystals is much weaker than that in the $(NH_4)_4H_2(SeO_4)_3$ and $(ND_4)_4D_2(SeO_4)_3$ crystals. The shift of the transition temperature is 17 K upward for the $Na_3H(SO_4)_2$ crystal on the substitution with deuterium. But no shift of the transition temperature is observed for the $(NH_4)_4H_2(SeO_4)_3$ crystal in the present studies. Therefore, it implies that the shift of the transition temperature by the substitution of deuterium in the hydrogen bonds is strongly affected by the magnitude of the bonding strength. Thus we suggest that there is a strong connection between the shift of the transition temperature and the bonding strength of the asymmetric O–H–O hydrogen bonds as suggested for the $(NH_4)_4H_2(SeO_4)_3$ and $Na_3H(SO_4)_2$ crystals. However, it is necessary to investigate more compounds which include the asymmetric O–H–O hydrogen bond to get a general conclusion.

References

[1] T. Fukami, R.H. Chen, *Phys. Status Solidi B* **214,** 219 (1999).

[2] Cz. Pawlaczyk, F.E. Salman, A. Pawlowski, *Phase Transit.* **8,** 9 (1986).

[3] Cz. Pawlaczyk, A. Pawlowski, *Phys. Status Solidi A* **113,** 447 (1989).

[4] M. Pavel, A. Pawlowski, Z. Zikmund, M. Drozdowski, *Solid State Ion.* **91,** 161 (1996).

[5] M. Polomska, W. Megist, A. Pawlowski, *Ferroelectrics Lett.* **20,** 63 (1995).

[6] M. Polomska, A. Pawlowski, *Ferroelectrics* **185,** 107 (1996).

[7] M. Polomska, *J. Mol. Struct.* **404,** 181 (1997).

[8] A.I. Kruglik, M.A. Simonov, *Sov. Phys.-Crystallogr.* **22,** 617 (1977).

[9] T. Fukami, R.H. Chen, *Solid State Commun.* **112,** 213 (1999).

[10] T. Fukami, N. Higa, R.H. Chen, *Acta Phys. Pol. A* **97,** 663 (2000).

[11] B.A. Frenz, *SDP for Windows Reference Manual*, Associates, Inc, College, Station, TX, 1995.

[12] M. Ichikawa, *Acta Crystallogr. B* **34,** 2074 (1978).

[13] M. Ichikawa, *Ferroelectrics* **168,** 177 (1995).

[14] M. Ichikawa, *J. Mol. Struct.* **552,** 63 (2000).

[15] M. Catti, G. Ferraris, G. Ivaldi, *Acta Crystallogr. B* **35,** 525 (1979).

[16] W. Joswig, H. Fuess, *Acta Crystallogr. B* **38,** 2798 (1982).

[17] T. Fukami, R.H. Chen, *Ferroelectrics* **211,** 67 (1998).

[18] T. Fukami, R.H. Chen, *Phys. Status Solidi B* **216,** 917 (1999).